

Landau quantization and neutron emissions by nuclei in the crust of a magnetar

N Chamel¹, Y D Mutafchieva², Zh K Stoyanov², L M Mihailov³ and R L Pavlov²

¹ Institute of Astronomy and Astrophysics, Université Libre de Bruxelles, CP 226, Boulevard du Triomphe, B-1050 Brussels, Belgium

² Institute for Nuclear Research and Nuclear Energy, Bulgarian Academy of Sciences, 72 Tsarigradsko Chaussee, 1784 Sofia, Bulgaria

³ Institute of Solid State Physics, Bulgarian Academy of Sciences, 72 Tsarigradsko Chaussee, 1784 Sofia, Bulgaria

E-mail: nchamel@ulb.ac.be

Abstract. Magnetars are neutron stars endowed with surface magnetic fields of the order of $10^{14} - 10^{15}$ G, and with presumably much stronger fields in their interior. As a result of Landau quantization of electron motion, the neutron-drip transition in the crust of a magnetar is shifted to either higher or lower densities depending on the magnetic field strength. The impact of nuclear uncertainties is explored considering the recent series of Brussels-Montreal microscopic nuclear mass models. All these models are based on the Hartree-Fock-Bogoliubov method with generalized Skyrme functionals. They differ in their predictions for the symmetry energy coefficient at saturation, and for the stiffness of the neutron-matter equation of state. For comparison, we have also considered the very accurate but more phenomenological model of Dufo and Zuker. Although the equilibrium composition of the crust of a magnetar and the onset of neutron emission are found to be model dependent, the quantum oscillations of the threshold density are essentially universal.

1. Introduction

At the end point of stellar evolution, neutron stars are not only the most compact stars in the universe, but also the strongest magnets [1]. In particular, magnetic fields of the order of $10^{14} - 10^{15}$ G have been measured at the surface of soft gamma-ray repeaters and anomalous x-ray pulsars [2], thus dubbed *magnetars*. On the other hand, numerical simulations have shown that the internal magnetic field could be even stronger, up to about 10^{18} G [3]. The outermost layer of a neutron star is thought to consist of a solid crust, whose atoms are fully ionized by the gravitational pressure (for a review, see Ref. [4]). With increasing depth, nuclei become progressively more neutron rich by capturing electrons until at some point, neutrons start to drip out of nuclei. The presence of a neutron liquid in the crust of a magnetar is expected to leave its imprint on various observed astrophysical phenomena like sudden spin-ups [5, 6] and spin-downs [7, 8, 9, 10] (generally referred to as “glitches” and “anti-glitches” respectively), quasiperiodic oscillations detected in the giant flares from soft gamma-ray repeaters [11, 12, 13] and cooling [14].

We have recently studied the effects of a strong magnetic field on the neutron-drip transition in the crust of a magnetar [15, 16]. We have shown that the neutron-drip density and pressure

increase almost linearly with the magnetic field strength in the strongly quantizing regime. In the weakly quantizing regime, the variations of the neutron-drip density with magnetic field strength exhibit typical quantum oscillations. The neutron-drip transition in a magnetar, as compared to unmagnetized neutron stars, can thus be shifted to either higher or lower densities depending on the magnetic field strength. In this paper, we explore the role of nuclear uncertainties on the neutron-drip transition considering different nuclear mass models.

2. Neutron emission in dense magnetized matter

During the gravitational collapse of the core of massive stars (whose mass lies in the range $\sim 8 - 10 M_\odot$, where M_\odot is the mass of the Sun), it is generally assumed that all kinds of reactions can occur so that the hot dense matter constituting the newly born neutron star remains in thermodynamic equilibrium. Eventually the neutron star interior becomes cold and fully “catalyzed” [1]. Although the temperature inside mature neutron stars with an age $\sim 10^4 - 10^5$ years is typically of the order of $10^7 - 10^8$ K, matter is so highly degenerate that for most practical purposes the temperature can be set to zero. Since the pressure inside the star must vary continuously, and since the temperature is fixed, the suitable thermodynamic potential for determining the internal composition of a neutron star is the Gibbs free energy per nucleon g (this still remains the case even in the presence of a strong magnetic field, as shown in Ref. [17]). In the deep region of the outer crust on which we focus, atoms are fully ionized by the pressure, and electrons can be treated as an almost ideal Fermi gas. The main correction arises from the electrostatic lattice energy (for a discussion of various other corrections, see e.g. Ref. [17]). In each layer at pressure P , the crust is assumed to be made of only one type of ions with proton number Z and mass number A , arranged on a body-centred cubic lattice. Due to the presence of a strong magnetic field B , the electron motion perpendicular to the field is quantized into Landau levels. The magnetic field $B_\star = B/B_{\text{crit}}$ can be conveniently measured in units of the critical magnetic field defined by

$$B_{\text{crit}} = \left(\frac{m_e c^2}{\alpha \lambda_e^3} \right)^{1/2} \simeq 4.4 \times 10^{13} \text{ G}, \quad (1)$$

where m_e is the electron mass, c the speed of light, α is the fine structure constant, and λ_e is the electron Compton wavelength. Typically, Landau quantization effects on the composition of the crust are negligible unless $B_\star \gg 1$. Further details on our crust model can be found in Refs. [15, 16].

In any region of the outer crust, the pressure is provided by the degenerate electron gas so that the electron chemical potential μ_e increases with depth until it reaches the threshold for neutron drip [16]

$$\mu_e(n_e, B_\star) + \frac{4}{3} C e^2 n_e^{1/3} Z^{2/3} = \mu_e^{\text{drip}}(A, Z), \quad (2)$$

where n_e is the electron number density, e is the proton electric charge, $C \approx -1.444$ is the body-centred cubic lattice structure constant, and

$$\mu_e^{\text{drip}}(A, Z) \equiv \frac{-M(A, Z)c^2 + A m_n c^2}{Z} + m_e c^2, \quad (3)$$

with $M(A, Z)$ the nuclear mass (including the rest mass of Z protons, $A - Z$ neutrons and Z electrons¹), and m_n the neutron mass. The equilibrium nucleus is found by minimizing the Gibbs free energy per nucleon. As discussed in Ref. [18], this nucleus is actually stable against

¹ The reason for including the electron rest mass in $M(A, Z)$ is that experimental *atomic* masses are generally tabulated rather than *nuclear* masses.

neutron emission, but unstable against electron captures accompanied by neutron emission. Equation (2) must be generally solved numerically. Nevertheless, an analytical solution can be obtained in the strongly quantizing regime for which electrons lie in the lowest Landau level and are ultrarelativistic ($\mu_e \gg m_e c^2$). In such case, the neutron-drip density and pressure are approximately given by [16]

$$n_{\text{drip}} \approx \frac{A B_\star \mu_e^{\text{drip}}(A, Z)}{Z \frac{2\pi^2 \lambda_e^3 m_e c^2}{3}} \left[1 - \frac{4}{3} C \alpha Z^{2/3} \left(\frac{B_\star}{2\pi^2} \right)^{1/3} \left(\frac{m_e c^2}{\mu_e^{\text{drip}}(A, Z)} \right)^{2/3} \right], \quad (4)$$

$$P_{\text{drip}} \approx \frac{B_\star \mu_e^{\text{drip}}(A, Z)^2}{4\pi^2 \lambda_e^3 m_e c^2} \left[1 - \frac{1}{3} C \alpha Z^{2/3} \left(\frac{4B_\star}{\pi^2} \right)^{1/3} \left(\frac{m_e c^2}{\mu_e^{\text{drip}}(A, Z)} \right)^{2/3} \right], \quad (5)$$

For any given magnetic field, the composition of the outer crust and the onset of neutron drip are completely determined by nuclear masses. The nuclei expected to be found in the bottom layers of the outer crust are so neutron rich that their masses have not yet been measured. For this reason, nuclear models must be employed. We have made use of the recent series of Brussels-Montreal microscopic nuclear mass models [19, 20]. These models are based on the self-consistent Hartree-Fock-Bogoliubov (HFB) method using generalized Skyrme functionals (see e.g. Ref. [21] for a review of the latest Brussels-Montreal models). These models were primarily fitted to the 2353 measured masses of nuclei with N and $Z \geq 8$ from the 2012 Atomic Mass Evaluation [22], with a root-mean square deviation $\sim 0.5 - 0.6$ MeV. At the same time, the underlying BSk functionals were constrained to reproduce various properties of infinite homogeneous nuclear matter, most of which are summarized in Table 1. These parameters are defined by first writing the energy per nucleon of nuclear matter of density n and charge asymmetry $\eta = (n_n - n_p)/n$ (n_n and n_p are the neutron and proton densities respectively) in the form

$$e(n, \eta) \approx e(n, \eta = 0) + e_{\text{sym}}(n) \eta^2, \quad (6)$$

in which the first term on the right-hand side is just the energy per nucleon of charge-symmetric nuclear matter; we have neglected charge-symmetry breaking terms, such as those arising from the neutron-proton mass difference. We then expand $e(n, \eta = 0)$ and $e_{\text{sym}}(n)$ about the equilibrium density n_0 in powers of $\epsilon = (n - n_0)/n_0$, thus

$$e(n, \eta = 0) \approx a_v + \frac{1}{18} K_v \epsilon^2, \quad (7)$$

and

$$e_{\text{sym}}(n) \approx J + \frac{1}{3} L \epsilon + \frac{1}{18} K_{\text{sym}} \epsilon^2. \quad (8)$$

For pure neutron matter ($\eta = 1$) at density n_0 , the pressure is approximately given by $P_n \approx L n_0/3$. Therefore, L is a measure of the stiffness of the neutron-matter equation of state. The functionals BSk22, BSk23, BSk24 and BSk25 were all fitted to the same realistic neutron-matter equation of state (as obtained from many-body calculations using realistic two- and three-nucleon forces), but were constrained to different symmetry energy coefficients, $J = 32, 31, 30$ and 29 MeV, respectively. BSk26 was constrained to the same symmetry-energy coefficient $J = 30$ MeV as BSk24, but was fitted to a softer neutron-matter equation of state. BSk27* yields the softest possible neutron-matter equation of state consistent with recent quantum Monte Carlo calculations and with the same symmetry-energy coefficient. The model HFB-27* is also the most accurate of this series. The range of values of J and L spanned by these functionals are consistent with constraints coming from the combined analysis of various experiments [23] (see also the discussion in Sec. IIIC in Ref. [19]). Moreover, the incompressibility coefficient

Table 1. Nuclear-matter properties predicted by recent Brussels-Montreal nuclear energy density functionals [19, 20].

	BSk22	BSk23	BSk24	BSk25	BSk26	BSk27*
n_0 [fm $^{-3}$]	0.1578	0.1578	0.1578	0.1587	0.1589	0.1586
a_v [MeV]	-16.088	-16.068	-16.048	-16.032	-16.064	-16.051
K_v	245.9	245.7	245.5	236.0	240.8	241.6
J [MeV]	32.0	31.0	30.0	29.0	30.0	30.0
L [MeV]	68.5	57.8	46.4	36.9	37.5	28.5
K_{sym} [MeV]	13.0	-11.3	-37.6	-28.5	-135.6	-221.4

K_v falls in the empirical range 240 ± 10 MeV [24]. Finally, the high-density equation of state of symmetric nuclear matter predicted by these functionals are compatible with the constraints inferred from the analysis of heavy-ion collision experiments [25, 26].

Taking the values of the nuclear masses from BRUSLIB [27], we have determined numerically the equilibrium composition of the outer crust of a magnetar for different magnetic field strengths. For comparison, we have also considered the more phenomenological model of Duflo and Zuker [28]. In the search of the equilibrium nucleus, we have made use of mass models only when experimental measurements from the 2012 Atomic Mass Evaluation [22] were not available. The composition at the neutron-drip transition is indicated in Table 2. For all models but HFB-22, the equilibrium nucleus is the same with or without the presence of a strong magnetic field. For model HFB-22, the equilibrium nucleus is found to be either ^{122}Kr or ^{128}Sr , depending on the magnetic field strength. The reason lies in the fact that the threshold electron chemical potentials μ_e^{drip} for these two nuclides differ by less than 0.2%. As shown in Figs. 1 and 2, the oscillations of the neutron-drip density as a function of B_\star are almost universal. In particular, in the presence of a nonquantizing magnetic field (i.e. more than one Landau level is populated), the shifts in the neutron-drip density are bounded, both from above and from below. The limits are approximately given by [16]:

$$\frac{n_{\text{drip}}^{\text{min}}}{n_{\text{drip}}(B_\star = 0)} \approx \frac{3}{4}, \quad (9)$$

$$\frac{n_{\text{drip}}^{\text{max}}}{n_{\text{drip}}(B_\star = 0)} \approx \frac{1}{72} (35 + 13\sqrt{13}). \quad (10)$$

3. Conclusions

We have pursued our study of the effects of Landau quantization on the onset of neutron emission by nuclei in the crust of a magnetar [16]. In particular, we have explored the impact of nuclear uncertainties considering the recent series of Brussels-Montreal Hartree-Fock-Bogoliubov nuclear mass models, from HFB-22 to HFB-27* [19, 20]. These models yield equally good fits to essentially all experimental masses, with a root-mean-square deviation of about 0.5 – 0.6 MeV. However, they lead to different predictions of nuclear-matter properties thus reflecting the current lack of knowledge of the symmetry energy, and the stiffness of the neutron-matter equation of state. For comparison, we also considered the more accurate but also more phenomenological model of Duflo and Zuker [28]. Although the equilibrium nucleus at the bottom the outer crust, and the onset of neutron emission are found to be model dependent, the oscillations of the threshold density as a function of the magnetic field strength are almost

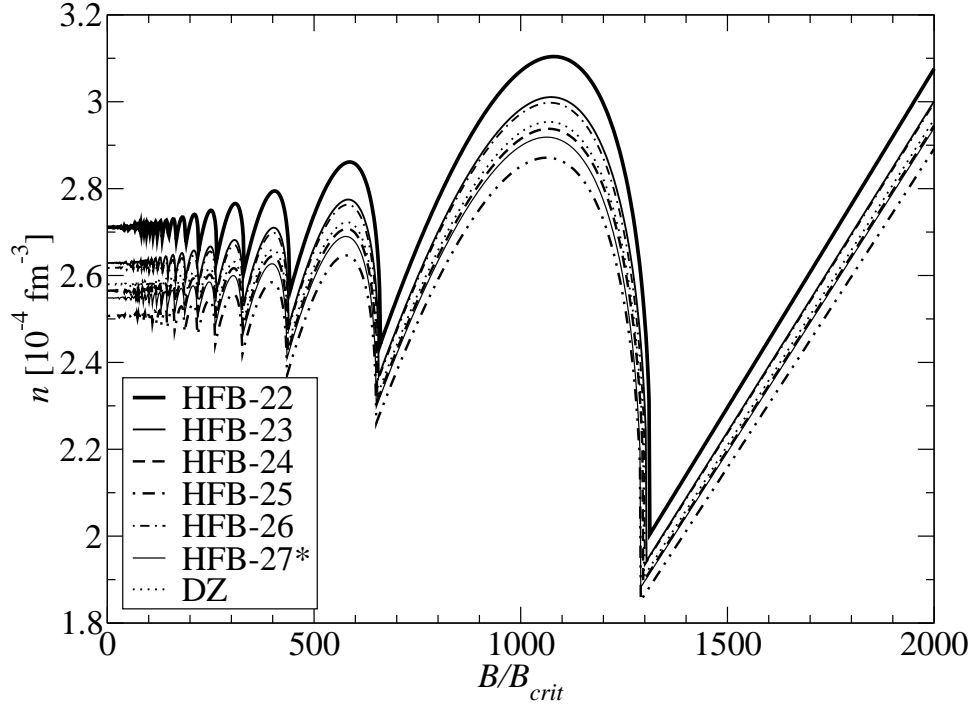


Figure 1. Threshold baryon number density for the onset of neutron drip in the crust of a neutron star as a function of magnetic field strength, as predicted by different nuclear mass models.

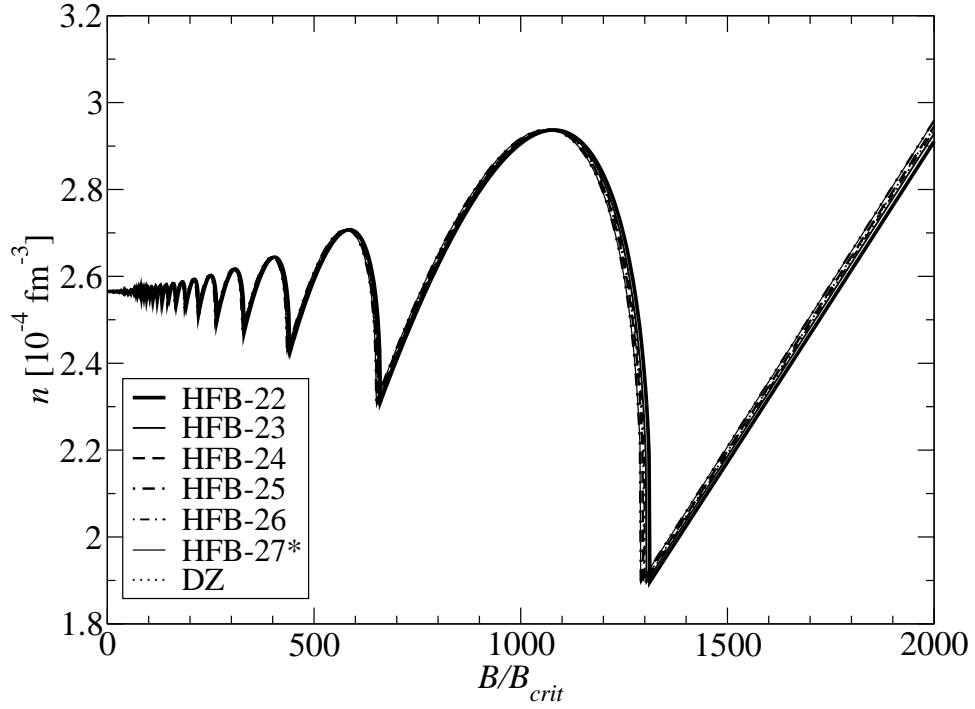


Figure 2. Same as Figure 1 after a suitable rescaling of the threshold density to that of HFB-24.

Table 2. Equilibrium nucleus and electron chemical potential at the neutron-drip transition in the crust of a magnetar, as predicted by different nuclear mass models.

	$A\text{X}$	μ_e^{drip} (MeV)
HFB-22	$^{122}\text{Kr}/^{128}\text{Sr}$	24.97/25.01
HFB-23	^{126}Sr	24.88
HFB-24	^{124}Sr	24.81
HFB-25	^{122}Sr	24.76
HFB-26	^{126}Sr	24.85
HFB-27*	^{124}Sr	24.76
DZ	^{118}Kr	24.87

universal. The role of the magnetic field on the neutron-drip density in magnetar crusts could thus be a priori inferred from the value of the neutron-drip density in unmagnetized neutron star crusts. On the other hand, the change of nuclear masses due to the strong magnetic field [29], which we have not taken into account, may undermine this universal behaviour.

Acknowledgments

This work was financially supported by Fonds de la Recherche Scientifique - FNRS (Belgium), Wallonie-Bruxelles-International (Belgium), the Bulgarian Academy of Sciences, the Bulgarian National Science Fund under contract No. DFNI-T02/19, and the European Cooperation in Science and Technology (COST) Action MP1304 “NewCompStar”.

References

- [1] Haensel P, Potekhin A Y, Yakovlev D G 2007 *Neutron Stars 1: Equation of state and structure* (Springer)
- [2] Olausen S A and Kaspi V M 2014 *Astrophys. J. Suppl. Ser.* **212** 6.
<http://www.physics.mcgill.ca/~pulsar/magnetar/main.html>
- [3] Chatterjee D, Elghozi T, Novak J and Oertel M 2015 *Mon. Not. R. Astron. Soc.* **447** 3785
- [4] Chamel N and Haensel P 2008 *Living Rev. Relativity* **11** 10. <http://www.livingreviews.org/lrr-2008-10>
- [5] Dib R, Kaspi V M and Gavril F P 2008 *Astrophys. J.* **673** 1044
- [6] Gügercinoglu E and Alpar A 2014 *Astrophys. J.* **788** L11
- [7] Archibald R A, Kaspi V M, Ng C -Y, Gourgouliatos K N, Tsang D, Scholz P, Beardmore A P, Gehrels N and Kennea J A 2013 *Nature* **497** 591
- [8] Şaşmaz Muş S, Aydın B and Göğüş E 2014 *Mon. Not. R. Astron. Soc.* **440** 2916
- [9] Duncan R C 2013 *Nature* **497** 574
- [10] Kantor E M and Gusakov M E 2014 *Astrophys. J.* **797** L4
- [11] Andersson N, Glampedakis K and Samuelsson L 2009 *Mon. Not. R. Astron. Soc.* **396** 894
- [12] Chamel N., Page D and Reddy S 2013 *Phys. Rev. C* **87** 035803
- [13] Passamonti A and Lander S K 2014 *Mon. Not. R. Astron. Soc.* **438** 156
- [14] Aguilera D N, Cirigliano V, Pons J A, Reddy S, Sharma R 2009 *Phys. Rev. Lett.* **102** 091101
- [15] Chamel N, Pavlov R L, Mihailov L M, Velchev Ch J, Stoyanov Zh K, Mutafchieva Y D, Ivanovich M D, Pearson J M and Goriely S 2012 *Phys. Rev. C* **86** 055804
- [16] Chamel N, Stoyanov Zh K, Mihailov L M, Mutafchieva Y D, Pavlov R L, Velchev Ch J 2015 *Phys. Rev. C* **91** 065801.
- [17] Chamel N and Fantina A F 2015 *Phys. Rev. D* **92** 023008
- [18] Chamel N, Fantina A F, Zdunik J L and Haensel P 2015 *Phys. Rev. C* **91** 055803
- [19] Goriely S, Chamel N and Pearson J M 2013 *Phys. Rev. C* **88** 024308
- [20] Goriely S, Chamel N and Pearson J M 2013 *Phys. Rev. C* **88** 061302(R)
- [21] Chamel N, Pearson J M, Fantina A F, Ducoin C, Goriely S and Pastore A 2015 *Acta Phys. Pol. B* **46** 349
- [22] Audi G, Wang M, Wapstra A H, Kondev F G, MacCormick M, Xu X and Pfeiffer B 2012 *Chin. Phys. C* **36** 002

- [23] Fantina A F, Chamel N, Pearson J M and Goriely S 2015 *AIP Conf. Proc.* **1645** 92
- [24] Colò G, Giai N V, Meyer J, Bennaceur K and Bonche P 2004 *Phys. Rev. C* **70** 024307
- [25] Danielewicz P, Lacey R and Lynch W G 2002 *Science* **298** 1592
- [26] Lynch W G, Tsang M B, Zhang Y, Danielewicz P, Famiano M, Li Z and Steiner A W 2009 *Progress in Particle and Nuclear Physics* **62** 427
- [27] <http://www.astro.ulb.ac.be/bruslib>
- [28] Duflo J and Zuker A P 1995 *Phys. Rev. C* **52** 23 (R)
- [29] Basilico D, Peña Arteaga D, Roca-Maza X and Coló G 2015 *Phys. Rev. C* **92** 035802